

Harmonic chains and the thermal diode effect

Na'im Kalantar,¹ Bijay Kumar Agarwalla,² and Dvira Segal^{3,4,*}

¹*Department of Chemistry, University of Toronto,
80 Saint George St., Toronto, Ontario, Canada M5S 3H6*

²*Department of Physics, Dr. Homi Bhabha Road,
Indian Institute of Science Education and Research, Pune, India 411008*

³*Department of Chemistry and Centre for Quantum Information and Quantum Control,
University of Toronto, 80 Saint George St., Toronto, Ontario, Canada M5S 3H6*

⁴*Department of Physics, University of Toronto, Toronto, Ontario, Canada M5S 1A7*

(Dated: November 19, 2021)

Harmonic oscillator chains connecting two harmonic reservoirs at different constant temperatures cannot act as thermal diodes, irrespective of structural asymmetry. However, here we prove that perfectly harmonic junctions can rectify heat once the reservoirs (described by white Langevin noise) are placed under temperature gradients, which are asymmetric at the two sides, an effect that we term “temperature-gradient harmonic oscillator diodes”. This nonlinear diode effect results from the additional constraint—the imposed thermal gradient at the boundaries. We demonstrate the rectification behavior based on the exact analytical formulation of steady state heat transport in harmonic systems coupled to Langevin baths, which can describe quantum and classical transport, both regimes realizing the diode effect under the involved boundary conditions. Our study shows that asymmetric harmonic systems, such as room-temperature hydrocarbon molecules with varying side groups and end groups, or a linear lattice of trapped ions may rectify heat by going beyond simple boundary conditions.

I. INTRODUCTION

Energy transport processes play central roles in chemical reactivity, biological function, and the operation of mechanical, electronic, thermal, and thermoelectric devices^{1–3}. Understanding energy transport in both the classical and quantum regimes is fundamental to thermodynamics, relaxation dynamics, chemical reactivity, and biomolecular dynamics^{3–5}.

Linear, one dimensional (1D) chains of particles and springs serve to model vibrational (phononic) heat transport through molecular chains. The force field, the functional form of the potential energy and its parametrization is often constructed by hand, such as in the eminent FPU model, to represent basic harmonic and anharmonic interactions^{6,7}. In molecular simulations, the force field is taken from first-principle (DFT) calculations⁸. Recent experiments probed the flow of vibrational energy (heat) through self-assembled monolayers of alkanes^{9–11} down to a single molecular junction^{12,13}. These junctions comprise a linear (quasi 1D) molecule bridging two solids with the steady state thermal heat current or the thermal conductance as observables of interest.

When the temperature is low relative to the characteristic vibrational frequencies, the harmonic force field can be adopted to model interactions in molecules since atomic displacements stay close to equilibrium. However, the harmonic potential leads to several intriguing, anomalous properties: Heat current in harmonic chains was calculated in both the classical¹⁴ and quantum^{15,16} regimes displaying an anomalous thermal conductivity that was diverging with size, in disagreement with the phenomenological-macroscopic Fourier’s law of heat conduction⁴.

Purely harmonic systems connecting harmonic baths at fixed temperatures T_H and T_C cannot support the thermal diode effect: The heat current is exactly symmetric upon exchange of temperatures between the heat source and drain, as directly observed from the Landauer formula for heat conduction^{4,15,16}. Recent studies realized a diode effect in harmonic junctions—by making parameters to be temperature-dependent—thus sensitive to the direction of the thermal bias¹⁷. Fundamentally, such effective harmonic models emerge due to underlying nonlinear interactions.

The thermal diode (rectifier) effect had been demonstrated in numerous 1D chains by combining anharmonic interactions and spatial asymmetry starting from Refs.^{21,22}. In one type of modelling, the chain is made of different segments and the diode effect can be explained due to the mismatch in the phonon spectral density in the forward and backward temperature-bias directions. Thermal rectifiers were further proposed in other models based on classical^{23–25} and quantum transport equations^{25–30}, with recent efforts dedicated to achieving high rectification ratios that persist with length^{31–34}.

At the nanoscale, the key ingredients of a thermal diode realized with harmonic reservoirs are (i) structural asymmetry, e.g. by using graded materials and (ii) anharmonicity of the force field^{5,35,36}. Anharmonicity in the form of a two-state system^{26,27} can be readily realized in hybrid models with an impurity³⁶ or spin chains coupled to boson baths^{37,38} (as well as in the opposite scenario of a boson chain coupled to spin baths³⁹); recent experiments demonstrated heat rectification with Josephson junction qubits^{40,41}.

In contrast, in molecules such as alkane chains the harmonic force field dominates interactions at room temper-

ature. Therefore, these molecules do not realize a noticeable diode effect in a steady state solid-molecule-solid configuration when constant temperatures (T_H and T_C) are maintained at the boundaries¹⁵. Pump-probe transient spectroscopy experiments demonstrated unidirectional vibrational energy flow between different chemical groups (e.g., nitro and phenyl)^{42,43}; corresponding observations of steady state asymmetric heat flow through molecules are still missing⁴⁴.

Can harmonic systems support the diode effect? In this paper, our goal is to revisit the problem of steady state heat transfer in asymmetric harmonic junctions and make clear the conditions for the realization of a thermal diode effect. In our model all components are harmonic: the reservoirs, representing e.g. solids, the chain (molecule), and their couplings. Furthermore, we do not effectively include anharmonicity by making parameters temperature dependent. As we had just discussed, microscopic harmonic chains that bridge two harmonic solids, a heat source and a heat drain at constant temperatures T_H and T_C , respectively, as depicted in 1(a)-(b), cannot act like a diode irrespective of structural asymmetry. However, once we modify the boundary condition as we show in Fig. 1(c) and impose *thermal gradients* in the contact region, the junction can *rectify* heat due to the (multi-affinity) boundary conditions, with particles directly coupled to different baths.

We exemplify this scenario, referred to as the temperature-gradient harmonic oscillator (TGHO) chain in Fig. 1(c). The hot solid is divided into several regions with externally controlled temperatures, $T_1^H > T_2^H > T_3^H$. Similarly, the colder region may be divided into domains with externally-controlled temperatures. This setup can be realized experimentally by controlling local temperatures (as in trapped-ions chain in optical lattices⁴⁶), or computationally, as a mean to introduce thermal gradients in structures, the result of genuine inelastic scatterings.

Our analysis is performed using formally-exact expressions for the heat current based on the quantum Langevin equation⁴. Both classical and quantum harmonic diodes are demonstrated, with quantum effects leading to an improved performance of the TGHO diodes. Furthermore, we describe a unique, purely-quantum TGHO diode, which does not have a classical analogue. As for classical diodes, we perform classical molecular dynamics (MD) simulations of heat flow in anharmonic junctions to demonstrate the extent of the diode effect under explicit anharmonicity in comparison to the TGHO diode.

Altogether, in this work we: (i) Derive conditions for realizing a new type of thermal diodes, the TGHO diode based on structural asymmetry and inhomogeneous temperature boundary conditions, (ii) identify a purely-quantum TGHO diode, (iii) make clear conditions for realizing thermal diodes in either genuine or effective harmonic models.

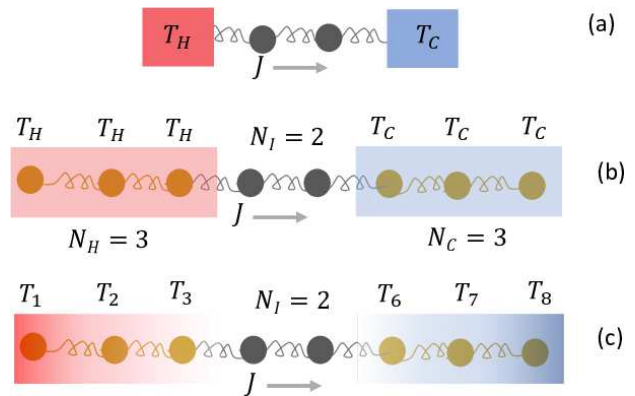


FIG. 1. (a) N -particle chain connecting two heat baths (modeled by Langevin thermostats), hot and cold, with bead 1 connected to the hot bath and bead N coupled to the cold one. In this example, $N = 2$. (b)-(c) N -site chain made of $N_H + N_C$ exterior beads coupled to Langevin heat baths and N_I particles in the central, interior zone. The imposed temperature at the edges may be homogeneous as in (b), or inhomogeneous as in (c), the latter potentially realizing a TGHO diode. In (b)-(c), we used $N = 8$ total number of beads.

II. MODEL AND METHOD: LINEAR CHAIN COUPLED TO HEAT BATHS

A. Model

We focus on a 1D harmonic oscillator chain with a total of N beads. The chain is coupled at its edges to two thermostats, also referred to as solids. In simulations of heat transport through solid-molecule-solid junctions, typically, rather than including the solids' atoms explicitly, they are emulated through Langevin baths to which the first and last atoms of the molecule are attached, see Fig. 1(a). This setup was considered in numerous computational studies, see e.g.^{4,15,27}, and since the system as a whole is microscopically harmonic, it cannot support the diode effect.

Let us now consider a more complex picture of a junction with *several* beads on each side (N_H , N_C) each attached to an independent Langevin noise term. The N_I interior particles are not thermostated. For example, in Fig. 1(b)-(c) we display an $N = 8$ -bead chain where atoms 1, 2 and 3 coupled to hot baths, while beads 6, 7, and 8 connected to colder reservoirs. We can think about this scenario in two different ways: We may regard all N beads as part of the molecular system, with the heater and sink reservoirs (implemented via Langevin noise) acting on several edge sites. Alternatively, we can picture this setup as a molecule made of the N_I interior beads only (4 and 5), with the modelling of the thermal reservoirs enriched: The solids are described by N_H and N_C physical beads, each connected to an independent Langevin bath. In fact, this latter approach has been adopted in molecular dynamics simulations of thermal conductance of nanoscale systems. It allows to engineer

a nontrivial phonon spectral function within a standard (white noise) Langevin simulation method⁴⁷.

What about the temperatures imposed at the boundaries? We consider two cases: (i) The temperature is homogeneous at the edges, $T_H = T_{1,2,3}$ and $T_C = T_{6,7,8}$. That is, beads 1, 2, and 3 are coupled to three independent Langevin baths, but each is maintained at the same temperature (and similarly for the cold side). This scenario is depicted in Fig. 1(b). (ii) A temperature profile is implemented at the edges: beads 1, 2, and 3 are coupled to Langevin baths with a *thermal gradient* such that the temperature of the attached baths follow the trend $T_1 > T_2 > T_3 > T_4 > T_5 > T_6$, see Fig. 1(c). It is not required that all temperatures vary; at minimum we require two affinities (three baths of different temperatures). We refer to this scenario as the temperature gradient harmonic-oscillator chain.

In what follows, we show that these two cases are *fundamentally* distinct. In the first setup, Fig. 1(b), a diode effect *cannot* show up even under structural asymmetries; remember that we work with harmonic oscillators. In contrast, in the second scenario, Fig. 1(c), a diode effect develops in both the classical and quantum regimes when the gradients are distinct and structural asymmetry is introduced. Moreover, we show that in a certain setup, a TGHO chain can support a purely-quantum diode—with no corresponding classical analogue.

B. Langevin equation formalism

We write down the classical Hamiltonian and corresponding classical equations of motion (EOM); a quantum description based on Heisenberg EOM directly follows⁴,

$$H = \sum_{i=1}^N \frac{p_i^2}{2m_i} + \frac{1}{2} \sum_{i=1}^{N+1} k_{i-1} (x_i - x_{i-1} - a)^2. \quad (1)$$

Here, x_0 and x_{N+1} are fixed, setting the boundaries. a is the equilibrium distance between nearest-neighbor sites.

At this stage, we assume that every particle i is coupled to an independent heat bath. This coupling is incorporated using the Langevin equation with a friction constant γ_i and stochastic forces $\xi_i(t)$ obeying the fluctuation-dissipation relation associated with exchanging energy with a heat bath, $\langle \xi_i(t) \xi_{i'}(t') \rangle = 2T_i \gamma_i \delta(t - t') \delta_{i,i'}$. In the model for the diode below, we specify the interior region (which is not thermostated) by setting its friction constants to zero. However, the TGHO effect is generic and can be discussed even when every bead is attached to a thermostat.

The classical EOM for the displacements are

$$m_i \ddot{x}_i = -k_{i-1} (x_i - x_{i-1} - a) + k_i (x_{i+1} - x_i - a) - \gamma_i v_i + \xi_i(t), \quad (2)$$

with v_i as the velocity of the i th particle.

The steady state heat current can be evaluated inside the chain by calculating heat exchange between beads, or at the contact region with each bath. Using the latter approach, the classical (C) heat current from bath l to its attached bead is ($k_B \equiv 1$, $\hbar \equiv 1$),⁴

$$J_l^C = \sum_m \gamma_l \gamma_m \int_{-\infty}^{\infty} d\omega \frac{\omega^2}{\pi} |(G(\omega))_{l,m}|^2 (T_l - T_m). \quad (3)$$

The summation is done over every thermostat. In what follows, we introduce the compact notation

$$M_{lm} \equiv \gamma_l \gamma_m \int_{-\infty}^{\infty} d\omega \frac{\omega^2}{\pi} |(G(\omega))_{l,m}|^2, \quad (4)$$

and write down $J_l^C = \sum_m M_{lm} (T_l - T_m)$.

It can be shown that Eq. (3) generalizes in the quantum (Q) case to⁴

$$J_l^Q = \sum_m \gamma_l \gamma_m \int_{-\infty}^{\infty} d\omega \frac{\omega^3}{\pi} |(G(\omega))_{l,m}|^2 [n_l(\omega) - n_m(\omega)], \quad (5)$$

with $n_l(\omega) = [e^{\omega/T_l} - 1]^{-1}$, the Bose-Einstein distribution function of bath l of temperature T_l . Here, $\mathbf{G}(\omega)$ is a symmetric matrix. The matrix $\mathbf{G}^{-1}(\omega)$ for the five-site model that we simulate below is given in Appendix A.

To calculate the net heat current, we separate the heat baths into two groups, N_H heat sources placed to the left of the interior region, and N_C heat sinks at the other side. The total input heat power is

$$J = \sum_{l=1}^{N_H} J_l, \quad (6)$$

and it equals the total output heat current at the colder baths.

We now reiterate that a thermal diode effect cannot appear in harmonic chains coupled to heat baths at two different temperatures (single affinity setup). If N_H beads are coupled to heat baths at T_H and similarly, N_C beads are attached to reservoirs at temperature T_C , the net quantum heat current is given by $J^Q = \sum_{l \in N_H} \sum_{m \in N_C} \gamma_l \gamma_m \int d\omega \frac{\omega^3}{\pi} |(G(\omega))_{l,m}|^2 [n_H(\omega) - n_C(\omega)]$. This expression is symmetric under the exchange of temperatures even if long range interactions are included so that $\mathbf{G}(\omega)$ is a full matrix. Thus, this setup cannot support a diode effect. The multi-affinity scenario is discussed in the next section.

III. TGHO DIODES

In this Section, we describe the principles behind the TGHO diode. We begin by exemplifying this effect in an $N = 5$ -bead chain depicted in Fig. 2, then we generalize the discussion to longer systems. As a case study, we set

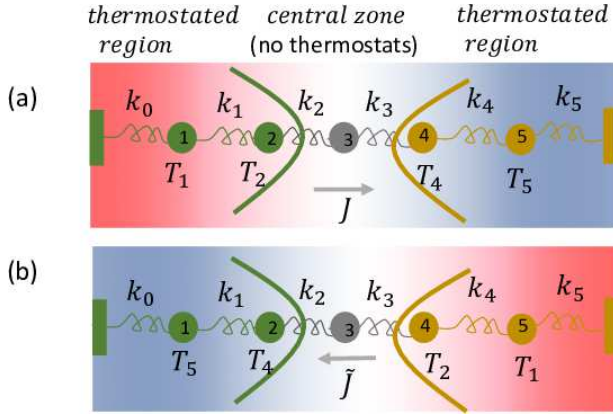


FIG. 2. A thermal rectifier based on an $N = 5$ -bead harmonic chain. Two beads at the boundaries are considered part of the solids, and they directly exchange energy with Langevin thermostats. (a) In the forward direction we set $T_1 > T_2 > T_4 > T_5$ and calculate the total heat input J from the baths attached to sites 1 and 2. (b) In the backward direction we interchange the temperatures such that bead 1 (2) is now attached to a thermal bath at temperature T_5 (T_4), and similarly for the other half. In this case we calculate the total heat input \tilde{J} from the hot baths, attached now to beads 4 and 5.

$N_I = 1$, $N_H = N_C = 2$; beads 1 and 2 are connected to hot baths, beads 4 and 5 are coupled to colder reservoirs, the central bead 3 is not thermostated. This separation is arbitrary and in practice should be based on the physical structure.

We begin with the classical (C) limit, Eq. (3). The total heat input in the forward (J) direction, corresponding to the setup of Fig. 2(a) is

$$J^C = (T_1 - T_4)M_{14} + (T_2 - T_5)M_{25} + (T_1 - T_5)M_{15} + (T_2 - T_4)M_{24}. \quad (7)$$

Reversing the temperature profile as in Fig. 2(b), $T_1 \leftrightarrow T_5$ and $T_2 \leftrightarrow T_4$, the reversed (\tilde{J}) current is

$$\tilde{J}^C = (T_5 - T_2)M_{14} + (T_4 - T_1)M_{25} + (T_5 - T_1)M_{15} + (T_4 - T_2)M_{24}. \quad (8)$$

The sum of the opposite currents, which quantifies the diode effect is

$$\Delta J \equiv J^C + \tilde{J}^C = [(T_1 - T_2) - (T_4 - T_5)](M_{14} - M_{25}). \quad (9)$$

We can now identify the necessary conditions for realizing the diode effect, $\Delta J \neq 0$: (i) The temperature gradients should be *distinct at the two boundaries*, $(T_1 - T_2) \neq (T_4 - T_5)$. (ii) The setup should include a spatial asymmetry such that $M_{14} \neq M_{25}$. Asymmetry should be introduced in the thermostated region, as we prove next. Explicitly, assuming the friction constants are uniform, $\gamma_{1,2,4,5} = \gamma$,

we get (Appendix A):

$$M_{14} = \frac{\gamma^2}{\pi} \int_{-\infty}^{\infty} d\omega \omega^2 \frac{|k_1 k_2 k_3 (-\omega^2 + i\gamma\omega + k_4 + k_5)|^2}{|\det \mathbf{G}^{-1}|^2} \\ M_{25} = \frac{\gamma^2}{\pi} \int_{-\infty}^{\infty} d\omega \omega^2 \frac{|k_2 k_3 k_4 (-\omega^2 + i\gamma\omega + k_0 + k_1)|^2}{|\det \mathbf{G}^{-1}|^2}. \quad (10)$$

Therefore, asymmetry in the central zone (see definitions in Fig. 2), in the form $k_2 \neq k_3$ cannot lead to the required asymmetry $M_{14} \neq M_{25}$, since these terms are not sensitive to the asymmetry. For the diode effect to hold, structural asymmetry must be included in the *thermostated zones*. For example, it could be introduced in the form $k_1 = k_0 \neq k_4 = k_5$. In appendix A we consider chains of arbitrary size N_I , with $N_H = N_C = 2$ and prove that structural asymmetry must be introduced within the thermostated zones to realize a diode.

Furthermore, in a chain of length N with N_B beads in each thermostated zone,

$$J^C = \sum_{i=1}^{N_B} \sum_{j=1}^{N_B} (T_i - T_{N+1-j}) M_{i,N+1-j} \\ \tilde{J}^C = \sum_{i=1}^{N_B} \sum_{j=1}^{N_B} (T_{N+1-i} - T_j) M_{i,N+1-j}. \quad (11)$$

Therefore,

$$\Delta J = \sum_{i=1}^{N_B} \sum_{j \neq i}^{N_B} [(T_i - T_j) + (T_{N+1-i} - T_{N+1-j})] M_{i,N+1-j} \quad (12)$$

Physically, the two asymmetries (structural and in the applied thermal gradients) are achievable in molecular junctions by connecting a molecule to distinct solids: Different materials are characterized by different phonon properties such that the force constants at the left side would be distinct from those at the right side, leading to the required spatial asymmetry (ii). Furthermore, given that different materials are employed at the two sides, it is reasonable to assume that a total imposed gradient ΔT would be divided unevenly on the two boundary regions such that condition (i) is satisfied. (In real materials, these gradients develop due to lattice anharmonicity.) Most importantly, we reiterate that imposing structural asymmetry ($k_2 \neq k_3$ in Fig. 2) while using identical boundaries ($k_0 = k_1 = k_4 = k_5$) cannot result in thermal rectification in our model.

In Appendix B, we discuss the corresponding TGHO diode effect for harmonic chains with local trapping (pinning) potentials. We show that the TGHO diode effect can develop only once pinning potentials at the two thermostated regions are different—applying as well unequal thermal gradients. This setup could correspond to a linear chain of trapped ions as described in Refs.^{19,20}

We now discuss several aspects of TGHO chains:

(i) **Absence of rectification with two affinities.** If the beads at the thermostated segments are coupled to equal-temperature baths, $T_1 = T_2$ and $T_4 = T_5$ in Fig. 2, then $\Delta J = 0$ irrespective of structural asymmetry implemented via e.g. mass gradient, differing force constants or couplings to the baths.

We emphasize that rectification does not develop in this single-affinity scenario even when the model is made more complex, e.g. by making the statistics of the baths quantum, including long-range (yet harmonic) interactions, or by allowing the baths to couple to all beads (with different strengths). This observation emerges from the analytic structure of the Landauer heat current expression.

(ii) **Classical and quantum TGHO diodes.** As we showed in Eq. (9), $\Delta J \neq 0$ once the gradients are different, $(T_1 - T_2) \neq (T_4 - T_5)$, unless a mirror symmetry is imposed with $M_{14} = M_{25}$. To break the symmetry between M_{14} and M_{25} , the thermostated regions should be made structurally asymmetric, i.e. $k_1 \neq k_4$

(iii) **Purely-quantum TGHO diode.** In the quantum limit, the temperatures in Eq. (9) appear within the Bose-Einstein distribution functions, included in the frequency integral. In this case, as long as at least three affinities are applied, e.g. $T_1 > T_2 > T_4 > T_5$, and even when the gradients are equal, $(T_1 - T_2) = (T_4 - T_5)$, thermal rectification would show up (assuming structural asymmetry is included as required.)

(iv) **Self consistent reservoir method.** The TGHO system is distinct from the self consistent reservoir (SCR) method, which was discussed in e.g. Refs.^{48–53} in the context of thermal rectification in quantum chains. The role of the SCRs is to mimic anharmonicity. These fictitious thermal baths are attached to *interior* beads while demanding zero net heat flow from the physical system to the SCRs. The temperature of the SCRs is dictated by this condition. In contrast, in the TGHO chain the thermostats are responsible for the power input and output from the system, and their temperature is freely assigned as independent boundary conditions.

IV. SIMULATIONS

A. Classical and Quantum TGHO diodes

Rectification effect can be measured in different ways, with $\Delta J \neq 0$, defined in Eq. (9), or based on a rectification ratio, $R \equiv |J/\tilde{J}|$. We demonstrate the TGHO diode effect in Fig. 3, where we study the effect in the 5-bead system corresponding to Fig. 2. We implement spatial asymmetry by using different force constants, $k_0 = k_1 \neq k_4 = k_5$. The current was calculated as the total input heat (6) (confirmed to be identical to the total heat dissipated to the cold baths) by numerically integrating Eqs. (3) and (5) with a fine frequency grid up to a cutoff frequency larger than all other energy scales. For a discussion of the subtleties of the heat

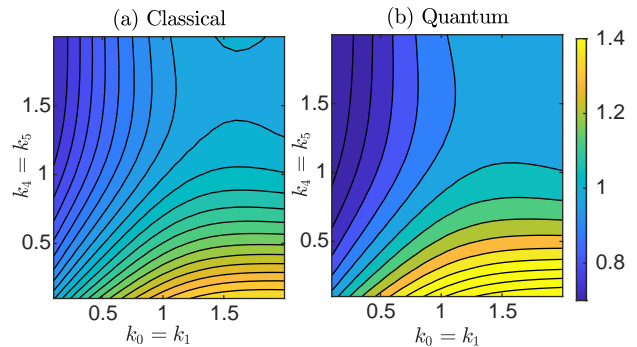


FIG. 3. Contour plot of the rectification ratio in an $N = 5$ -particle harmonic chain with $N_H = N_C = 2$. (a) Classical case and (b) quantum calculation with $T_1 = 1$, $T_2 = 0.5$, $T_4 = 0.2$, $T_5 = 0.1$ and $\gamma = 1$; the central bead is not coupled to a thermostat. We introduce different harmonic force constants at the thermostated regions, but use $k_2 = k_3 = 1$ for the interior part, masses are set at $m = 1$.

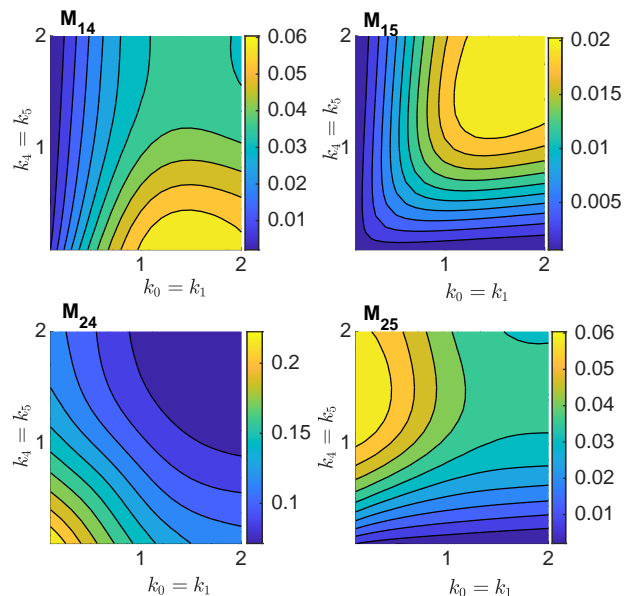


FIG. 4. The elements M_{ij} for the classical model corresponding to simulations in Fig. 3. Rectification arises due to the asymmetry $M_{14} \neq M_{25}$. Parameters are the same as in Fig. 3.

current definition see⁵⁴.

We show that both classical and quantum calculations can create the diode effect. In Fig. 3(a), the rectification ratio reaches up to $R \approx 1.4$ in both the classical and quantum cases. While the effect is not very large, it is in fact comparable to rectification ratios emerging due to an anharmonic potential, as we discuss below in Fig. (8). In Fig. 3(b) we display the behavior of the quantum TGHO diode, indicating on a somewhat stronger diode effect (bottom-right domain).

How can we tune the system to increase the rectification ratio? As can be seen from the analytic form of the

heat current for a 5-bead chain, there are four terms that play a role in the rectification ratio, M_{14} , M_{25} , M_{15} and M_{24} . These contributions are displayed in Fig. 4. We conclude that at large asymmetry (bottom-right part), M_{14} should dominate—once the gradients are made large. At this region, roughly $R \approx |(T_1 - T_4)/(T_5 - T_2)|$, which is ≈ 2 in our parameters, close to the achieved maximal rectification ratio of 1.4.

Thus, a viable strategy to increase rectification is to impose large structural asymmetry between the two ends, as well as apply significantly-unequal thermal gradients at the left and right side. The large spatial asymmetry results in the the dominance of a single transport pathway. Furthermore, by imposing a large gradient at the left side, ΔT_H , and a small gradient at the right side, ΔT_C , with a small temperature drop on the central region (such that in the example used, $T_4 \sim T_2$) the rectification ratio of the model scales as $R \propto |\Delta T_H / \Delta T_C|$. Below (Fig. 7) we further show that in long chains, the rectification effect is suppressed with $N_B = N_{H,C}$, but it only weakly depend on N_I . We therefore suggest that $R \propto \frac{1}{N_B} \left| \frac{\Delta T_H}{\Delta T_C} \right|$.

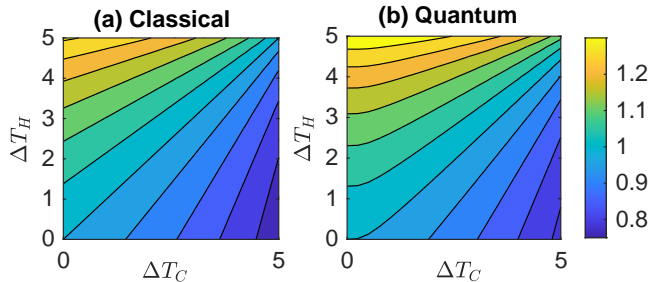


FIG. 5. Dependence of rectification on the temperature differences $\Delta T_H = T_1 - T_2$ and $\Delta T_C = T_4 - T_5$ in (a) classical and (b) quantum calculations. Rectification is enhanced when one gradient is very large and the other small. Here, $T_1 = 10$, $T_2 = 10 - \Delta T_H$, $T_4 = \Delta T_C$, $T_5 = 0$. The force constants are $k_0 = k_1 = 2$, $k_2 = k_3 = 1$, $k_4 = k_5 = .1$, $m = 1$ and $\gamma = 1$.

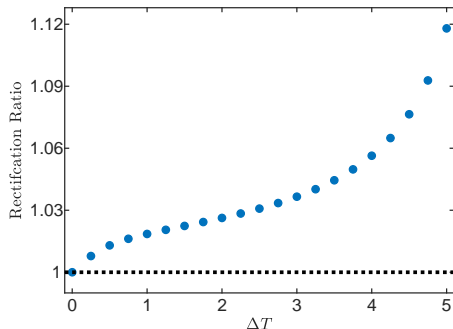


FIG. 6. Purely-quantum TGHO diode operating when the thermal gradients at the two boundaries are equal, $\Delta T_H = \Delta T_C$; we display the diagonal of Fig. (5). Parameters are $T_1 = 10$, $T_2 = 10 - \Delta T$, $T_4 = \Delta T$, $T_5 = 0$.

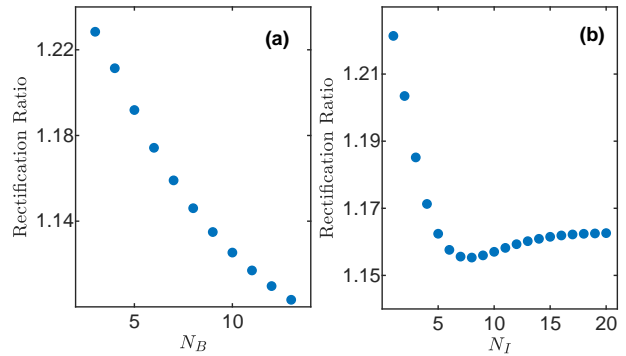


FIG. 7. Behavior of the rectification ratio with (a) N_B , number of thermostated sites, and (b) N_I , number of interior sites. We set temperatures and gradients as $T_1 = 1$, $T_2 = 0.5$, $T_4 = 0.2$, $T_5 = 0.1$ thus $\Delta T_H = 1 - 0.5$ and $\Delta T_C = 0.2 - 0.1$. In panel (a), a linear gradient is assumed within each thermostated region. In panel (b), $N_H = N_C = 2$. Other parameters are $\gamma = 1$, and force constants in the left (right) thermostated region at 1 (.1); other constants are set to 1. Simulations were performed using classical expressions.

B. Purely-quantum TGHO diode

The dependence of the classical and quantum TGHO diode effect on the local gradients is presented in Fig 5. As described above, the diode effect is enhanced when e.g. the left side experiences a large thermal gradient, while temperatures at the right side are almost identical. The classical case cannot support the diode effect when the local gradients are equal, $\Delta T_H = \Delta T_C$. In contrast, quantum statistics allows the diode behavior under equal gradients. This effect is illustrated in the behavior along the diagonal of Fig. 5(b), presented for clarity in Fig. 6.

C. Length dependence of the TGHO diode effect

Fig. (7) displays the behavior of the rectification ratio as the size of the system increases. In panel (a) we increase the number of thermostated sites N_B while fixing the overall temperature differences ΔT_H and ΔT_C , assuming a linear gradient in each region. We find that rectification decays as the number of thermostated sites increases. In contrast, the rectification ratio persists and saturates as we increase the number of sites in the interior region, N_I . This saturation is expected since in harmonic chains thermal transport is ballistic. Thus, the impact of the central region on the the rectification effect should become independent of length, N_I for long enough chains.

D. Comparison to an anharmonic diode

To appreciate the magnitude of the rectification effect in the TGHO chain, we present in Fig. (8) the diode behavior emerging when anharmonic interactions are explicitly added to the chain. We use the Frenkel-Kontorova (FK) potential that was used in many demonstrations of nonlinear thermal devices, e.g.,^{22,55,56}, adding onsite potentials to Eq. (1),

$$V(x) = V_{R/L} \cos\left(\frac{2\pi}{a}x\right). \quad (13)$$

Specifically, for the five-site chain, we encode asymmetry in the force constants and in the local potentials, V_L vs. V_R . Unlike the harmonic case, which is analytically solvable, to treat anharmonic interactions we turn to numerical molecular dynamics simulations. The Langevin equations of motion are integrated with the Brünger-Brooks-Karplus method; simulations were performed by propagating the dynamics long enough to reach a steady state, then finding the heat current by averaging the local currents between adjacent beads. Here we compute heat current as the net power exchanged between central beads, $\langle J^C \rangle = \frac{k_2}{2} \langle (v_2 + v_3)(x_3 - x_2 - a) \rangle$. We then average over time and over realizations of the noise. Technical details were discussed in Ref.⁵⁴. Results are presented in Fig. (8). Note that in the FK calculation, we resort to the standard modelling with a single thermal affinity, T_H at the left thermostat and T_C at the right side. Furthermore, only the leftmost (bead 1) and rightmost (N) beads are thermostated,

Comparing Fig. (8) to e.g. Fig. (3), we note that rectification in the anharmonic FK model is comparable to values received in the TGHO diode. Thus, while the rectification ratio demonstrated with the TGHO chain model is not impressive, is similar to what one would achieve using similar parameters in the FK anharmonic chain, a central model for diodes examined in the literature. The FK model has been optimized to show large rectification ratio²²; similarly, it is interesting to explore means for enhancing the TGHO diode effect.

V. DISCUSSION AND SUMMARY

We described a new type of a thermal diode, which is constructed in a purely-harmonic system when attached to multiple thermostats, thus imposing at least two affinities. The TGHO diode operates when two conditions are met: The thermostated regions are (i) structurally asymmetric with respect to each other and (ii) placed under unequal thermal gradients. We further proved the onset of a purely-quantum TGHO diode, which exists when the reservoirs (of different temperatures) are placed under equal gradients. We analyzed the dependence of the TGHO diode effect on chain length and the applied temperature gradient and further compared its performance

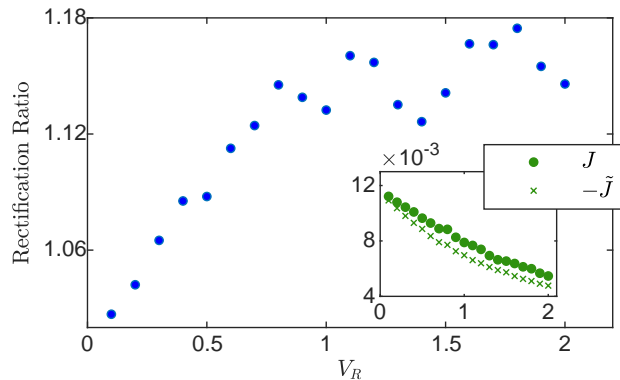


FIG. 8. Rectification ratio in the Frenkel-Kontorova anharmonic chain. The setup is analogous to Fig. (1)(a) with the leftmost and rightmost particles thermostated. Rectification is achieved by adding different anharmonic onsite FK potentials to the left (first two beads) and right (last three beads) sides of the five-bead chain. Here, at the right side, $V_R = 1$ and $k = 1$ while at the other half of the chain V_L varies and $k = 0.1$. Other parameters are $T_H = 1$, $T_C = .1$, $\gamma = 1$. The inset presents the currents in the forward (J) and reversed (\tilde{J}) directions.

to a diode model that was based on an anharmonic force field.

Recent studies used harmonic junctions with a single affinity (as in Figs. 1(a)-(b)) to realize a diode effect^{19,20}; this was achieved by making parameters such as friction coefficients temperature dependent, $\gamma_1(T)$, $\gamma_N(T)$. We refer to such models as effective harmonic-oscillator diodes. In this case, going back for simplicity to the classical limit, Eq. (3), the net heat current is given by $J \propto (T_H - T_C)\gamma_1(T_H)\gamma_N(T_C)M_{1N}(T_H, T_C)$, where we extracted the friction coefficients from the definitions of M_{1N} in Eq. (4). Assuming e.g. a linear dependence of friction coefficients with the temperature of the attached bath, $\gamma_{1,N}(T_H) = \gamma_{1,N} + \lambda(T_H - T_C)$, and $\gamma_{1,N}(T_C) = \gamma_{1,N} - \lambda(T_H - T_C)$, with λ as the slope, one obtains a diode effect,

$$\Delta J \propto \lambda(T_H - T_C)^2(\gamma_N - \gamma_1)M_{1N}(T_H, T_C), \quad (14)$$

where for simplicity we assumed that the friction coefficients have a small effect on the the Green's function $G(\omega)$. The diode effect $\Delta J \neq 0$ relies on two conditions: (i) structural asymmetry in the form here of $\gamma_1 \neq \gamma_N$, and (ii) hidden-effective interactions $\lambda \neq 0$, making parameters temperature dependent. Notably, this effective harmonic oscillator diode scales quadratically with the temperature difference, $\Delta J \propto (T_H - T_C)^2$. This quadratic scaling is the fingerprint of a hidden anharmonicity, illustrating a nonlinear phenomena. In contrast, the TGHO diode is a linear effect, characterized by the linear scaling of the net heat current with local temperature biases, $\Delta J \propto \Delta T$, see Eq. (9).

Purely harmonic junctions connecting heat baths at two different temperatures cannot rectify heat. Our

Longer chains have the analogous property that force constants between beads not connected to heat baths play no role in rectification: Asymmetry must appear between the sections directly thermalized by baths. More precisely, in an N -bead chain with $N_H = N_C = 2$, so that beads 1, 2; $N - 1$, and N are connected to thermostats we get

$$\begin{aligned}\det(C_{1(N)}) &= k_1 k_{N-1} \left(\prod_{i=2}^{N-2} -k_i \right) \\ \det(C_{1(N-1)}) &= -k_1 \left(\prod_{i=2}^{N-2} -k_i \right) (-\omega^2 + i\gamma\omega + k_{N-1} + k_N) \\ \det(C_{2(N)}) &= -k_{N-1} \left(\prod_{i=2}^{N-2} -k_i \right) (-\omega^2 + i\gamma\omega + k_0 + k_1) \\ \det(C_{2(N-1)}) &= \left(\prod_{i=2}^{N-2} -k_i \right) (-\omega^2 + i\gamma\omega + k_0 + k_1)(-\omega^2 + i\gamma\omega + k_{N-1} + k_N)\end{aligned}\tag{A7}$$

Rectification appears when $\det(C_{1(N-1)}) \neq \det(C_{2(N)})$, thus $k_1 \neq k_{N-1}$ and/or $k_0 \neq k_N$; asymmetry in the central region force constants, k_2, \dots, k_{N-2} is not sufficient to enact rectification.

APPENDIX B: TGHO DIODE WITH ASYMMETRIC ONSITE POTENTIALS

In this Appendix we include asymmetry by introducing local trapping potentials with force constant \tilde{k} ; the

interparticle potentials are assumed identical. For the five-particle chain with harmonic onsite potentials, the inverse Green's matrix has form

$$\mathbf{G}^{-1}(\omega) = \begin{pmatrix} -\omega^2 + i\gamma\omega + 2k + \tilde{k}_1 & -k & & & & & & \\ -k & -\omega^2 + i\gamma\omega + 2k + \tilde{k}_2 & -k & & & & & \\ & -k & -\omega^2 + 2k + \tilde{k}_3 & -k & & & & \\ & & -k & -\omega^2 + i\gamma\omega + 2k + \tilde{k}_4 & -k & & & \\ & & & -k & -\omega^2 + i\gamma\omega + 2k + \tilde{k}_5 & & & \\ & & & & -k & -\omega^2 + i\gamma\omega + 2k + \tilde{k}_5 & & \end{pmatrix}$$

We again set $N_H = N_C = 2$ and $N_I = 1$; two beads are thermalized at each boundary, while the single bead at the centre (particle 3) is not thermalized. The diode effect for this system can be quantified by Eq. (9), and it is controlled by the asymmetry between M_{14} and M_{25} . We provide now explicit expressions for these terms to analyze the required source of asymmetry.

The elements $\det(C_{ij})$ take the form

$$\begin{aligned}\det(C_{15}) &= k^4, \\ \det(C_{14}) &= -k^3(-\omega^2 + i\gamma\omega + 2k + \tilde{k}_5), \\ \det(C_{25}) &= -k^3(-\omega^2 + i\gamma\omega + 2k + \tilde{k}_1), \\ \det(C_{24}) &= k^2(-\omega^2 + i\gamma\omega + 2k + \tilde{k}_1)(-\omega^2 + i\gamma\omega + 2k + \tilde{k}_5).\end{aligned}\tag{B1}$$

In this case, rectification can show up once $\tilde{k}_1 \neq \tilde{k}_5$ resulting in $M_{14} \neq M_{25}$. As in the case of asymmetric interparticle forces, this holds for chains of any size. For an N -bead chain with $N_H = N_C = 2$,

$$\begin{aligned}\det(C_{1(N)}) &= k^{N-1}, \\ \det(C_{1(N-1)}) &= -k^{N-2}(-\omega^2 + i\gamma\omega + 2k + \tilde{k}_N), \\ \det(C_{2(N)}) &= -k^{N-2}(-\omega^2 + i\gamma\omega + 2k + \tilde{k}_1), \\ \det(C_{2(N-1)}) &= k^{N-3}(-\omega^2 + i\gamma\omega + 2k + \tilde{k}_1)(-\omega^2 + i\gamma\omega + 2k + \tilde{k}_N).\end{aligned}\tag{B2}$$

Therefore, it is the asymmetry $\tilde{k}_1 \neq \tilde{k}_N$ that is responsi-

ble for the diode effect. Inspecting this form, we expect

that the TGHO chain with an asymmetry in the inter-

particle force constants would support larger rectification ratios than the case with pinning potentials.

-
- * dvira.segal@utoronto.ca
- ¹ I. V. Rubtsov and A. L. Burin, Ballistic and diffusive vibrational energy transport in molecules, *J. Chem. Phys. Perspective* **150**, 020901 (2018).
 - ² Thermal and thermoelectric properties of molecular junctions, K. Wang, E. Meyhofer, and P. Reddy, *Adv. Func. Mater.* **30**, 1904534 (2020).
 - ³ D. Segal and B. K. Agarwalla, Vibrational heat transport in molecular junctions, *Ann. Rev. Phys. Chem.* **67**, 185 (2020).
 - ⁴ A. Dhar, Heat transport in low dimensional systems, *Adv. Phys.* **57**, 457 (2008).
 - ⁵ D. M. Leitner, Quantum ergodicity and energy flow in molecules, *Adv. Phys.* **64**, 445 (2015).
 - ⁶ E. Fermi, J. Pasta and S. Ulam, Studies of nonlinear problems, Los Alamos Scientific Laboratory report LA-1940 (1955).
 - ⁷ T. Dauxois, Fermi, Pasta, Ulam, and a mysterious lady, *Physics Today* **61**, 55 (2008).
 - ⁸ J. C. Klöckner and F. Pauly, Variability of the thermal conductance of gold-alkane-gold single-molecule junctions studied using ab-initio and molecular dynamics approaches, arXiv:1910.02443.
 - ⁹ M. D. Losego, M. E. Grady, N. R. Sottos, D. G. Cahill, and P. V. Braun, Effects of chemical bonding on heat transport across interfaces, *Nat. Mater.* **11**, 502 (2012).
 - ¹⁰ T. Meier, F. Menges, P. Nirmalraj, H. Hölscher, H. Riel, and B. Gotsmann Length-dependent thermal transport along molecular chains, *Phys. Rev. Lett.* **113**, 060801 (2014).
 - ¹¹ S. Majumdar, J. A. Sierra-Suarez, S. N. Schiffres, W.-L. Ong, C. F. Higgs, A. J. H. McGaughey, and J. A. Malen, Vibrational mismatch of metal leads controls thermal conductance of self-assembled monolayer junctions, *Nano Lett.* **15**, 2985 (2015).
 - ¹² N. Mosso, H. Sadeghi, A. Gemma, S. Sangtarash, U. Drechsler, C. Lambert, and B. Gotsmann, Thermal transport through single-molecule junctions, *Nano Lett.* **19**, 7614 (2019).
 - ¹³ L. Cui, S. Hur, Z. A. Akbar, J. C. Klöckner, W. Jeong, F. Pauly, S. Y. Jang, P. Reddy, and E. Meyhofer, Thermal conductance of single-molecule junctions, *Nature* **572**, 628 (2019).
 - ¹⁴ Z. Rieder, J. L. Lebowitz, and E. Lieb, Properties of a Harmonic Crystal in a Stationary Nonequilibrium State, *J. Math. Phys.* **8**, 1073 (1967).
 - ¹⁵ D. Segal, A. Nitzan, and P. Hänggi, Thermal conductance through molecular wires, *J. Chem. Phys.* **119**, 6840 (2003).
 - ¹⁶ L. G. C. Rego and G. Kirczenow, Quantized thermal conductance of dielectric quantum wires, *Phys. Rev. Lett.* **81**, 232 (1998).
 - ¹⁷ A thermal diode effect can be realized in “effective” harmonic systems—once anharmonicity is introduced at a mean field level, by making parameters temperature dependent^{18–20}. In these type of models there is a cross-graining or mean-field assumption making parameters temperature dependent. In Ref.²⁰ for example the friction coefficient was varied with temperature, thus allowing the occurrence of a diode effect in an *effective* harmonic junction. To eliminate confusion, we highlight that here all parameters are temperature independent, and that the model is microscopically harmonic.
 - ¹⁸ E. Pereira, Requisite ingredients for thermal rectification, *Phys. Rev. E* **96**, 012114 (2017).
 - ¹⁹ M. A. Simon, S. Martinez-Garaot, M. Pons, and J. G. Muga, Asymmetric heat transport in ion crystals, *Phys. Rev. E* **100**, 032109 (2019).
 - ²⁰ M. A. Simón, A. Alaña, M. Pons, A. Ruiz-García, and J. G. Muga, Heat rectification with a minimal model of two harmonic oscillators, *Phys. Rev. E* **103**, 012134 (2021).
 - ²¹ M. Terraneo, M. Peyrard, and G. Casati, Controlling the energy flow in nonlinear lattices: A model for a thermal rectifier, *Phys. Rev. Lett.* **88**, 094302 (2002).
 - ²² B. Li, L. Wang, and G. Casati, Thermal Diode: Rectification of Heat Flux, *Phys. Rev. Lett.* **93**, 184301 (2004).
 - ²³ N. Li, J. Ren, L. Wang, G. Zhang, P. Hänggi, and B. Li, Colloquium: Phononics: Manipulating heat flow with electronic analogs and beyond, *Rev. Mod. Phys.* **84**, 1045 (2012).
 - ²⁴ M. Y. Wong, C. Y. Tso, T. C. Ho, and H. H. Lee, A review of state of the art thermal diodes and their potential applications *Int. J. Heat and Mass Transfer* **164**, 120607 (2021).
 - ²⁵ G. Benenti, G. Casati, C. Mejía-Monasterio, and M. Peyrard, From Thermal Rectifiers to Thermoelectric Devices. In: Lepri S. (eds) *Thermal Transport in Low Dimensions. Lecture Notes in Physics*, vol 921. Springer, Cham. 2016.
 - ²⁶ B. K. Agarwalla and D. Segal, Energy current and its statistics in the nonequilibrium spin-boson model: Majorana fermion representation, *New J. Phys.* **19**, 043030 (2017).
 - ²⁷ D. Segal and A. Nitzan, Spin-boson thermal rectifier, *Phys. Rev. Lett.* **94**, 034301 (2005).
 - ²⁸ E. Pereira, Thermal rectification in classical and quantum systems: Searching for efficient thermal diodes, *Europhys. Lett.* **126**, 14001 (2019).
 - ²⁹ D. M. Leitner, Thermal boundary conductance and thermal rectification in molecules *J. Phys. Chem. B* **117**, 12820 (2013).
 - ³⁰ K. M. Reid, H. D. Pandey, and D. M. Leitner, Elastic and inelastic contributions to thermal transport between chemical groups and thermal rectification in molecules, *J. Phys. Chem. C* **123**, 6526 (2019).
 - ³¹ S. Chen, E. Pereira, and G. Casati, Ingredients for an efficient thermal diode, *EPL* **111**, 30004 (2015).
 - ³² S. Chen, D. Donadio, G. Benenti, and G. Casati, Efficient thermal diode with ballistic spacer *Phys. Rev. E* **97**, 030101 (2018).
 - ³³ T. Alexander, High-heat-flux rectification due to a localized thermal diode, *Phys. Rev. E* **101**, 62122 (2020).
 - ³⁴ S. You, D. Xiong, and J. Wang, Thermal rectification in the thermodynamic limit, *Phys. Rev. E* **101**, 012125 (2020).

- ³⁵ S.-A. Wu and D. Segal, Sufficient conditions for thermal rectification in hybrid quantum structures, *Phys. Rev. Lett.* **102**, 095503 (2009).
- ³⁶ L.-A. Wu, C. X. Yu, and D. Segal, Nonlinear quantum heat transfer in hybrid structures: Sufficient conditions for thermal rectification, *Phys. Rev. E* **80**, 041103 (2009).
- ³⁷ S. H. S. Silva, G. T. Landi, R. C. Drumond, and E. Pereira, Heat rectification on the XX chain, *Phys. Rev. E* **102**, 062146 (2020).
- ³⁸ V. Balachandran, G. Benenti, E. Pereira, G. Casati, and D. Poletti, Heat current rectification in segmented XXZ chains, *Phys. Rev. E* **99**, 032136 (2019).
- ³⁹ V. Balachandran, S. R. Clark, J. Goold, and D. Poletti, Energy current rectification and mobility edges, *Phys. Rev. Lett.* **123**, 020603 (2019).
- ⁴⁰ J. Senior, A. Gubaydullin, B. Karimi, J. T. Peltonen, J. Ankerhold, and J. P. Pekola, Heat rectification via a superconducting artificial atom, *Comm. Phys.* **3**, 40 (2020).
- ⁴¹ A. Iorio, E. Strambini, G. Haack, M. Campisi, and F. Gizotto, Photonic heat rectification in a coupled qubits system, arXiv:2101.11936.
- ⁴² B. C. Pein, Y. Sun, and D. D. Dlott, Unidirectional vibrational energy flow in nitrobenzene, *J. Phys. Chem. A* **117**, 6066 (2013).
- ⁴³ B. C. Pein, Y. Sun, and D. D. Dlott, Controlling vibrational energy flow in liquid Alkylbenzenes, *J. Phys. Chem. B* **117**, 10898 (2013).
- ⁴⁴ Nanoscale solid-state thermal rectifiers were realized e.g. in Ref.⁴⁵ based on mass-graded carbon and boron nitride nanotubes.
- ⁴⁵ C. W. Chang, D. Okawa, A. Majumdar, and A. Zettl, Solid-state thermal rectifier, *Science* **314**, 1121 (2006).
- ⁴⁶ M. Ramm, T. Pruttivarasin, and H. Häffner, Energy transport in trapped ion chains, *New J. Phys.* **16**, 063062 (2016).
- ⁴⁷ I. Sharony, R. Chen, and A. Nitzan, Stochastic simulation of nonequilibrium heat conduction in extended molecule junctions, *J. Chem. Phys.* **153**, 144113 (2020).
- ⁴⁸ F. Bonetto, J. L. Lebowitz, and J. Lukkarinen, Fourier's Law for a harmonic crystal with self-consistent stochastic reservoirs, *J. Stat. Phys.* **116**, 783 (2004).
- ⁴⁹ E. Pereira and H. C. F. Lemos, Symmetry properties of heat conduction in inhomogeneous materials, *Phys. Rev. E* **78**, 031108 (2008).
- ⁵⁰ D. Segal, Absence of thermal rectification in asymmetric harmonic chains with self consistent reservoirs: An exact analysis, *Phys. Rev. E* **79**, 012103 (2009).
- ⁵¹ M. Bandyopadhyay and D. Segal, Quantum heat transfer in harmonic chains with self consistent reservoirs: Exact numerical simulations, *Phys. Rev. E* **84**, 011151 (2011).
- ⁵² E. Pereira, H. C. F. Lemos, and R. R. Ávila, Ingredients of thermal rectification: The case of classical and quantum self-consistent harmonic chains of oscillators, *Phys. Rev. E* **84**, 061135 (2011).
- ⁵³ R. Moghaddasi Fereidani and D. Segal, Phononic heat transport in molecular junctions: quantum effects and vibrational mismatch, *J. Chem. Phys.* **150**, 024105 (2019).
- ⁵⁴ N. Kalantar, B. K. Agarwalla and D. Segal, On the definitions and simulations of vibrational heat transport in nanojunctions, *J. Chem. Phys.* **153**, 174101 (2020).
- ⁵⁵ B. Li, L. Wang, and G. Casati, Negative differential thermal resistance and thermal transistor, *App. Phys. Lett.* **88**, 143501 (2006).
- ⁵⁶ L. Wang and B. Li, Thermal logic gates: computation with phonons, *Phys. Rev. Lett.* **99**, 177208 (2007).